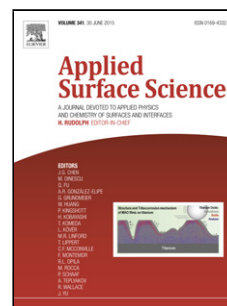# Accepted Manuscript

Title: Electrochemical properties of composite cathodes using Sm doped layered perovskite for intermediate temperature-operating solid oxide fuel cell

Authors: Seung-Wook Baek, Abul K. Azad, John T.S. Irvine, Won Seok Choi, Hyunil Kang, Jung Hyun Kim

Please cite this article as: Seung-Wook Baek, Abul K.Azad, John T.S.Irvine, Won Seok Choi, Hyunil Kang, Jung Hyun Kim, Electrochemical properties of composite cathodes using Sm doped layered perovskite for intermediate temperature-operating solid oxide fuel cell, Applied Surface Science http://dx.doi.org/10.1016/j.apsusc.2017.02.211

Electrochemical properties of composite cathodes using Sm doped layered perovskite for intermediate temperature-operating solid oxide fuel cell

Seung-Wook Baek [a], Abul K. Azad [b], John T. S. Irvine [c], Won Seok Choi [d], Hyunil Kang [d], Jung Hyun Kim [e,*]

[a] Center for Energy Materials Metrology, Division of Industrial Metrology, Korea Research Institute of Standards and Science (KRISS), 267 Gajeong-Ro, Yuseong-Gu, Daejeon 305-340, Republic of Korea

[b] Faculty of Integrated Technologies, University Brunei Darussalam, Jalan Tunku Link, Gadong, BE1410, Brunei Darussalam

[c] School of Chemistry, University of St.Andrews, St.Andrews, Fife, KY16, 9ST, United Kingdom

[d] Department of Electrical Engineering, Hanbat National University, 125, Dongseo-Daero, Yuseong-Gu, Daejeon 305-719, Republic of Korea

[e] Department of Advanced Materials Science and Engineering, Hanbat National University, 125, Dongseo-Daero, Yusung-Gu, Daejeon, 305-719, Republic of Korea

Corresponding author:*

Jung Hyun Kim: jhkim2011@hanbat.ac.kr, jhkim1870@gmail.com Tel: +82-42-821-1239,

Fax: +82-42-821-1592, Department of Advanced Materials Science and Engineering, Hanbat

National University, 125, Dongseo-Daero, Yusung-Gu, Daejeon, 305-719, Republic of Korea

Highlights

▶ The ASR properties using two types of electrolytes are investigated.

▶ SBCO50 showed the lowest ASR values in the overall temperature range.

▶ The percolation limit was also achieved for a SBCO50 composite cathode.

▶ SBCO50 on CGO91 has to be adopted at 750 $^{\circ}$C or in a lower temperature range

▶ SBCO50 on CGO91 coated 8YSZ has to be used as a temperature of 750 $^{\circ}$C of above.

Abstract

SmBaCo$_2$O$_{5+d}$ (SBCO) showed the lowest observed Area Specific Resistance (ASR) value

in the LnBaCo$_2$O$_{5+d}$ (Ln: Pr, Nd, Sm, and Gd) oxide system for the overall temperature ranges

tested. The ASR of a composite cathode (mixture of SBCO and Ce$_{0.9}$Gd$_{0.1}$O$_{2-d}$) on a

Ce$_{0.9}$Gd$_{0.1}$O$_{2-d}$ (CGO91) electrolyte decreased with respect to the CGO91 content; the

percolation limit was also achieved for a 50 wt% SBCO and 50 wt% CGO91 (SBCO50) composite cathode.

The ASRs of SBCO50 on the dense CGO91 electrolyte in the overall temperature range of 500 to 750 °C were relatively lower than those of SBCO50 on the CGO91 coated dense 8 mol % yttria-stabilized zirconia (8YSZ) electrolyte for the same temperature range. From 750 °C and for all higher temperatures tested, however, the ASRs of SBCO50 on the CGO91 coated dense 8YSZ electrolyte were lower than those of the CGO91 electrolyte.

The maximum power densities of SBCO50 on the Ni-8YSZ / 8YSZ / CGO91 buffer layer were 1.034 W cm^{-2} and 0.611 W cm^{-2} at 800 °C and 700 °C.

1. Introduction

Recently, Intermediate Temperature-operating Solid Oxide Fuel Cells (IT-SOFCs) have been focused on because Solid Oxide Fuel Cells (SOFCs) operated at high operating temperature ranges over 800 °C have problems of thermal degradation, thermal expansion mismatch and high fabrication cost. However, cathode overpotential has dramatically

increased at the intermediate operating temperature ranges and has typically been the major source of voltage loss in IT-SOFC operation. Therefore, most research on IT-SOFCs had been devoted to cathode materials [1–3].

One candidate cathode material using ionic and electronic conductors (MIECs), a layered perovskite with the general formula $LnBaCo_2O_{5+d}$ (Ln: lanthanides $0 < d < 1$), has recently been a subject of interest for cathode materials for IT-SOFCs because of its high oxygen transport properties, excellent oxygen surface exchange coefficients and superior oxide ionic diffusivity [4,5].

Our group has shown that layered perovskite materials are promising cathode materials for application to IT-SOFCs at temperatures between 500 ºC and 700 ºC [6-9]. For example, the maximum electrical conductivity value of SBCO was 570 S cm^{-1} at 200 ºC; this material also showed a metal–insulator transition (MIT) phenomenon at about 200 ºC. The Area Specific Resistance (ASR) results for single phase SBCO and for a composite cathode comprised of 50 wt% SBCO and 50 wt% CGO91 were 0.13 and 0.05 Ω cm^2 at 700 ºC. The coefficients of thermal expansion (CTE) of the SBCO of 19.7×10^{-6} K^{-1} and 20.0×10^{-6} K^{-1} at 600 and 700 ºC dropped to 12.5×10^{-6} K^{-1} and 12.7×10^{-6} K^{-1} at 600 and 700 ºC, which values are similar to the value of the CGO91 electrolyte [7].

In this work, the electrochemical properties of a composite cathode prepared using SBCO with various weight percentages of CGO91 (from 0 wt% to 70 wt%) were investigated for

direct application as IT-SOFC cathode material. Significantly, the ASR properties when using two types of electrolytes (CGO91 and CGO91 coated 8 mol% Y_2O_3 stabilized ZrO_2 (8YSZ)) are also investigated for the operating temperature conditions. In addition, the power densities when using a single phase cathode and composite cathodes on a Ni-8YSZ / 8YSZ / CGO91 buffer layer were also measured for cathode application of IT-SOFC.

2. Experimental

2.1. Sample preparation and phase synthesis

Layered perovskites with general chemical compositions of $LnBaCo_2O_{5+d}$ (Ln: lanthanides) were prepared by general solid state reaction using high purity oxides (Praseodymium oxide (Pr_6O_{11}, Aldrich, 99.9%), Neodymium oxide (Nd_2O_3, Aldrich, 99.9%), Samarium oxide (Sm_2O_3, Aldrich, 99.9%), Gadolinium oxide (Gd_2O_3, Aldrich, 99.9%) and Cobalt oxide (Co_3O_4, Aldrich, 99.9%)) and carbonate (barium carbonate, ($BaCO_3$, Aldrich, 99.9%)). These oxides and carbonate were heat-treated at 300 ºC for 2 hours to achieve dehydration of the raw materials. After weighing the powders for exact stoichiometry with respect to the molar ratio of lanthanide oxides, barium carbonate and cobalt oxide, the samples were calcined in two steps. In the case of the first calcination process, the powders were mixed and ground in a mortar and pestle. Then, in order to decompose the carbonate, they were placed in a muffle furnace and heated at various ramp rates from room temperature to 1000°C for 8 hours as a

first calcination. The temperature for the first calcination was increased in 3 steps, for example 300, to 500 to 750 $^{\circ}$C before reaching 1000 $^{\circ}$C. After finishing the cooling process to room temperature, the samples were ground and ball-milled for 24 hours with zirconia media in acetone. In the second step, samples were heated at 1100 $^{\circ}$C for 36 hours at an increment of 5 $^{\circ}$C/min and were then cooled to room temperature.

X-ray diffraction (XRD) patterns of the prepared samples were obtained in a Philips diffractometer using Cu radiation ($\lambda = 0.15418$ nm). The obtained data were matched with the reference data for identification of the crystal structures.

2.2. Half cell fabrication and test

For the fabrication of symmetric half cells that could be used to perform electrochemical characterizations, 10 mol% gadolinia doped ceria ($Ce_{0.9}Gd_{0.1}O_{2-d}$, CGO91, Praxair Specialty Ceramics, 99.9%) and 8 mol% Y_2O_3 stabilized ZrO_2 (8YSZ, Tosoh) were used as electrolytes. These electrolytes were prepared by pressing the powders into pellets with circular shapes at 2 x 10^3 kg/m^2 and sintering them at 1400°C for 4 hours. The final dimensions of the sintered CGO91 electrolyte pellets were approximately 21 mm diameter and 2 mm thickness. For the CGO91 buffer layer coated 8YSZ electrolyte, CGO91 slurry was prepared with vehicle systems comprised of α-Terpineol and Butvar, spin coated onto the surface of the sintered 8YSZ and then heat treated at 1300 $^{\circ}$C for 3 hours.

Single phase cathodes and composite cathodes with CGO91 powders were also used for

electrochemical measurements. Vehicle systems comprised of α-Terpineol and Butvar were prepared and then cathodes were mixed with vehicles. The characteristics of the initial single phase cathodes and of the composite phase cathodes are summarized in Table 1. These cathodes were coated onto the electrolytes using screen printing to form symmetrical half cells. These half cells were sintered for 1 h at 1000 °C in order to form a porous electrode structure well bonded to the electrolyte. The final surface area of the symmetric cells was about 1.09 cm^2.

Measurements of the ASRs of the cathodes were conducted in air at open circuit voltage (OCV) as a function of temperature between 500 and 850 ^{o}C, with an increment of 50 ^{o}C. An AC four-probe method using a Solartron 1260 was used to measure the electrochemical properties. Impedance measurements were conducted in a frequency range of 5 MHz to 100 mHz; the amplitude of the applied voltage was 20 mV under OCV. The ASRs, measured from the differences between the first intercept in the vicinity of the high frequency and the last intercept at low frequency, were divided in two because the tested cells had two symmetrical electrodes.

2.3. Single cell fabrication and test

Anode substrates of SOFC comprised of 8YSZ and NiO (Alfa, 99.9%) powders were provided by the Korea Electric Power Research Institute (KEPRI), as previously reported and as can be found in the literature [10]. After coating the CGO91 slurry on the anode substrates

of SOFC with a spin coater, a buffer layer (CGO91 slurry) coated sample was sintered at 1300 $^{\circ}$C for 3 hours. SmBaCo$_2$O$_{5+d}$ (SBCO) and 50 wt% SBCO-50 wt% CGO91 (SBCO50) cathodes were also screen-printed and then heat-treated on CGO91 coated anode substrates at 1000 °C for 1 hour.

Power densities multiplied by voltage and current were measured as a function of applied current density using a Solatron 1286 with a 4 lead configuration under 5% H$_2$ / N$_2$ from 600 $^{\circ}$C to 800 $^{\circ}$C with a water bubbling system. 3% H$_2$O humidified H$_2$ was supplied to the anode chamber by bubbling through deionized water at a flow rate of 100 sccm. Air was also fed into the cathode chamber as the oxidant gas. When supplying hydrogen gas and the oxidant gas, mass flow controllers were used to control the gas flow rates. Pt-paste and Pt-mesh were used for current collection. Pt mesh, having a surface area of 1.09 cm^2, was placed on the cathodes; Pt paste was also used between the mesh and each electrode as a current collector.

3. Results and discussion

3.1. Electrochemical properties of LnBaCo$_2$O$_{5+d}$

Fig. 1 shows the relationships of the Area Specific Resistances (ASRs) to the various lanthanide replacements in the LnBaCo$_2$O$_{5+d}$ (Ln: Pr, Nd, Sm, and Gd) oxide systems as a function of temperature in the range of 500 to 850 $^{\circ}$C. The ASRs of PrBaCo$_2$O$_{5+d}$ (PBCO) at 600, 650 and 700 $^{\circ}$C are 1.209, 0.475 and 0.233 Ω cm^2 and the values of NdBaCo$_2$O$_{5+d}$

(NBCO) in this same tested temperature range are 0.606, 0.438 and 0.259 Ω cm^2. In addition,

GdBaCo$_2$O$_{5+d}$ (GBCO) shows ASR values of 13.749, 4.943 and 1.945 Ω cm^2 at 600, 650 and

700 ^{o}C. Finally, the ASRs of SmBaCo$_2$O$_{5+d}$ (SBCO) in the same measured temperature range

are 0.603, 0.283 and 0.131 Ωcm^2. Consequently, from these summarized ASR values, as

well as from the results shown in Fig. 1, it can be asserted that the Sm doped layered

perovskite (SBCO) shows the lowest observed ASR values in the LnBaCo$_2$O$_{5+d}$ (Ln: Pr, Nd,

Sm, and Gd) oxide systems; therefore, Sm substitution in LnBaCo$_2$O$_{5+d}$ can play an important

role in decreasing ASR values.

However, most of the ASR values, except for the value of 0.131 Ω cm^2 of the SBCO

measured at 700 ^{o}C, are not below the target ASR value (0.15 Ω cm^2 at 700 ^{o}C) suggested by

Steel and Heinzel for cathode materials for IT-SOFC [11]. This low performance can be

improved by introducing the concept of a composite cathode to a single phase cathode; this is

a mixed structure using the cathode material of SBCO and the electrolyte material of CGO91.

Importantly, the usage of such composite cathodes can not only increase the ionic

conductivity but also extend the three phase boundary (TPB) between the cathode and the

electrolyte. In addition, the coefficient of thermal expansion (CTE) for such s structure

decreases as a function of the increased contents of electrolyte material [12-17].

3.2. Electrochemical properties of composite cathodes

9

The ASR values of single phase (SBCO) and composite cathodes with SBCO and CGO91 were investigated with respect to the temperature and CGO91 contents; results are summarized in Fig. 2 (a) and (b).   In the case of these experiments, the composite cathodes are denoted with initials. For example, SBCO40 is the composite cathode consisting of 60 wt % SBCO and 40 wt% CGO91. According to the order of abbreviation, SBCO50 is a sample with 50 wt % of SBCO and 50wt% of CGO91; SBCO70 is a composite cathode comprising of 30 wt % of SBCO and 70 wt% of CGO91.

These results are shown in Fig. 2 (a) and (b); the ASR results for SBCO, SBCO20, SBCO40 and SBCO50 were presented in our previous work in the literature [7]. The ASR values of SBCO10, SBCO30, SBCO60 and SBCO70, which have been also reported in the literature [8], are 0.155, 0.095, 0.093 and 0.133 Ω cm^2 at 700 ^{o}C. From the summarized results shown in Fig. 2 (b), it can be seen that the percolation limit was achieved for the SBCO50 composition and, significantly, the optimized triple phase boundary influenced the electrochemical processes, resulting in reduced polarization.

Fig. 3 shows the impedance plots of SBCO50 on dense CGO91 electrolyte with respect to the temperature tested. From these plots, it can be seen that the resistance caused by the grain boundary of CGO91 is between at 500 and 550 ^{o}C, in the vicinity of the high frequency ranges (10^3 Hz); this level of resistance is not observed after 600 ^{o}C. From the impedance results for SBCO50 on CGO91 electrolyte at temperatures over 600 ^{o}C, it can be seen that the

charge transfer occuring at the interface between the cathode and electrolyte is not dominant when the temperature increases, which indicates that the active site of the electrode and the electrolyte is extended as a result of the enhanced triple phase boundary (TPB).

Fig. 4 shows impedance results for SBCO and SBCO50, allowing a comparison with the ASR differences with respect to the CGO91 level of SBCO. The cathodic polarization of the two cathode materials is dependent on the CGO91 content; the cathodic polarization of SBCO50 is 50% lower than that of SBCO at all temperatures tested because of the enhanced active sites and the increased triple phase boundary in the electrodes. For example, the impedance results for the various composite cathodes with SBCO, SBCO20, SBCO40 and SBCO50 measured at 700 $^{\circ}$C show the relationship of the CGO91 content effect in these composite cathode systems. These results show not only the effect of CGO91 in the composite cathode but also explain the phenomenon of percolation. In summary, the usage of CGO91 as one of the components in a composite cathode improves the ionic conductivity and the mixed ionic and electronic (MIEC) property, as well as bringing about improvements in the oxygen diffusion rate at the boundary of the cathode and in the electrolyte and charge transfer of oxygen ions.

Impedance spectra of SBCO50 on CGO91 (buffer layer) coated 8YSZ from 500 to 750 $^{\circ}$C are shown in Fig. 5; the resistance of the grain boundary in 8YSZ can be found in the vicinity of 10^4 Hz, as high as the frequency ranges measured at 500 $^{\circ}$C. Therefore, in this case, it is

determined from the impedance spectra that the cathodic polarization of SBCO50 is in the frequency range of 10^4 Hz or less than 10^4 Hz. From these impedance results, the charge transfer resistance can be seen to affect the overall resistance when the temperature increases. In addition, when one compares Figs. 5 and 3 of the impedance plots, the separation of the entire impedance plot occurs due to the 8YSZ-based electrolyte.

In order to illustrate the CGO91 effect, Fig. 6 provides the summarized results for SBCO50 with different electrolytes, for example, the CGO91 coated 8YSZ electrolyte and the CGO91 electrolyte. In the temperature ranges tested, the total set of ASRs of SBCO50 on the CGO91 coated dense 8YSZ electrolyte in the overall temperature range of 500 to 750 ^{o}C were relatively larger than those of SBCO50 on the dense CGO91. However, the ASR value of SBCO50 is expected to be almost the same at 750 ^{o}C. From 750 ^{o}C to the higher temperature ranges tested, the ASRs of SBCO50 on the CGO91 electrolyte were higher than those of CGO91 coated 8YSZ. Therefore, it is desirable that SBCO50 on CGO91 be adopted in a temperature range of 750 ^{o}C or less and that SBCO50 on CGO91 coated 8YSZ be applied at a temperature of 750 ^{o}C or above. In addition, the differences between these electrolytes show the impact of the activation energy, although all use the same material (SBCO50). For example, the activation energy of SBCO50 on the CGO91 electrolyte is found to be approximately 1.06 eV. However, the value of SBCO50 on the CGO91 coated 8YSZ electrolyte was 1.40 eV.

3.3. Performance properties of single cell

Figure 7 shows the performances, as a function of applied current density, of single cells comprised of Ni-YSZ / YSZ / CGO91 (buffer layer)/ SBCO and Ni-YSZ / YSZ / CGO91 / SBCO50 under 5% H_2 / N_2 from 600 ^oC to 800 ^oC with a water bubbling system. The results, expressed in gray color, are from the SBCO50 as a composite cathode; the black color shows the results from SBCO as single phase cathode.

From these results, two galvanostatic single cell tests shows open circuit voltages (OCV) of 1.078 V for the SBCO cathode and 1.089 V for the SBCO50 cathode when measuring is performed at 800 ^oC; these values were very close to the values obtained using the Nernst equation with humidified hydrogen (3% H_2O) as fuel [18], which implies that the YSZ electrolyte was well formed, without pores or cracks on the Ni-YSZ anode substrate, and that the fuel gas did not pour out from the anode side during operation.

When comparing the power density values of the cathode materials on CGO91 coated 8YSZ, SBCO50 shows power density values of 1.034, 0.830, 0.611, 0.387 and 0.216 W cm^{-2} at 800, 750, 700, 650 and 600 ^oC, respectively. The performance reported here can be significantly improved by using humidified pure H_2 as a fuel and oxygen instead of the 5% H_2 / N_2 and air. In addition, the maximum power density values of SBCO with Ni-YSZ / YSZ / CGO91 (buffer layer) are 0.968, 0.684, 0.401, 0.211 and 0.105 W cm^{-2} at the temperature ranges shown in Fig.7. The increased power density implies that full coverage of the ionic

conduction phase has effectively extended the triple phase boundaries (TBPs) and consequently increased the electrochemical activity of the SBCO electrodes.

4. Conclusions

The Sm doped layered perovskite shows the lowest observed ASR values in $LnBaCo_2O_{5+d}$ (Ln: Pr, Nd, Sm, and Gd) oxide systems. When adding various weight percentages of CGO91 (0 wt% to 70 wt%) to single phase SBCO, SBCO50 comprised of 50 wt% of SBCO and 50wt% of CGO91 showed the lowest values in the overall temperature range. From the electrochemical results obtained using a variety of electrolytes, SBCO50 on CGO91 has to be adopted at 750 ^{o}C or in a lower temperature range and SBCO50 on CGO91 coated 8YSZ has to be used as a temperature of 750 ^{o}C of above. The maximum power densities of SBCO50 on the CGO91 buffer coated anode substrate were 1.034 W cm^{-2} and 0.611 W cm^{-2} at 800 ^{o}C and 700 ^{o}C.

Acknowledgements

References

[1] N.Q. Minh, Ceramic fuel cells, J. Am. Ceram. Soc. 76 (1993) 563-588.

[2] N.Q. Minh, T. Takahashi, Science and Technology of Ceramic Fuel Cell, Elsevier, New York, 1995, pp. 1-14.

[3] T. Tsai, S.A. Barnett, Effect of LSM-YSZ cathode on thin-electrolyte solid oxide fuel cell performance, Solid State Ionics 93 (1997) 207-217.

[4] G. Kim, S.Wang, A.J. Jacobson, L. Reimus, P. Brodersen, C.A. Mims, Rapid oxygen ion diffusion and surface exchange kinetics in $PrBaCo_2O_{5+x}$ with a perovskite related structure and ordered A cations, J. Mater. Chem. 17 (2007) 2500-2505.

[5] A. Tarancón, A. Morata, G. Dezanneau, S.J. Skinner, J.A. Kilner, S. Estradé, F. Hernández-Ramírez, F. Peiró, J.R.Morante, $GdBaCo_2O_{5+x}$ layered perovskite as an intermediate temperature solid oxide fuel cell cathode, J. Power Sources 174 (2007) 255-263.

[6] W.Z. Zhou, C.T.Lin, W.Y. Liang, Synthesis and structural studies of the perovskite-related compound $YBaCo_2O_{5+x}$, Adv. Mater. 5 (1993) 735-738.

[7] J.H. Kim, Y. Kim, P.A. Connor, J.T.S. Irvine, J. Bae, W. Zhou, Structural, thermal and electrochemical properties of layered perovskite $SmBaCo_2O_{5+d}$, a potential cathode material for intermediate-temperature solid oxide fuel cells, J. Power Sources 194 (2009) 704-711.

[8] J. H. Kim, J. Bae, M. Cassidy, P. A Connor, W. Zhou, J. T. S. Irvine, $SmBaCo_2O_{5+d}$ and $LnBa_{0.5}Sr_{0.5}Co_2O_{5+d}$ potential cathode materials for IT-SOFC, ECS Trans. 25 (2009) 2707-2715.

[9] J.H. Kim, M. Cassidy, J.T.S. Irvine, J. Bae, Advanced electrochemical properties of $LnBa_{0.5}Sr_{0.5}Co_2O_{5+\delta}$ (Ln = Pr, Sm, and Gd) as cathode materials for IT-SOFC, J. Electrochem. Soc. 156(6) (2009) B682-B689.

[10] J. Bae, S. Lim, H. Jee, J. H Kim, Y.-S. Yoo, T Lee, Small stack performance of intermediate temperature-operating solid oxide fuel cells using stainless steel interconnects and anode-supported single cell, J. Power Sources 172 (2007) 100-107.

[11] B.C.H. Steele, A. Heinzel, Materials for fuel-cell technologies, Nature 414 (2001) 345-352.

[12] E. Perry Murray, M. J. Sever, S. A. Barnett, Electrochemical performance of $(La,Sr)(Co,Fe)O_3$-$(Ce,Gd)O_3$ composite cathodes, Solid State Ionics 148 (2002) 27-34.

[13] A. Barbucci, R. Bozzo, G. Cerisola, P. Costamagna, Characterisation of composite SOFC cathodes using electrochemical impedance spectroscopy. Analysis of Pt/YSZ and LSM/YSZ electrodes, Electrochim. Acta 47 (2002) 2183-2188.

[14] M. J. Jørgensen, S. Primdahl, M. Mogensen, Characterisation of composite SOFC cathodes using electrochemical impedance spectroscopy, Electrochim. Acta 44, (1999) 4195-4201.

[15] M. J. L. Østergard, C. Clausen, C. Bagger, M. Mogensen, Manganite-zirconia composite cathodes for SOFC: Influence of structure and composition, Electrochim. Acta 40 (1995) 1971-1981.

[16] S. Wang, T. Kato, S. Nagata, T. Honda, T. Kaneko, N. Iwashita, M. Dokiya, Performance of a $La_{0.6}Sr_{0.4}Co_{0.8}Fe_{0.2}O_3$-$Ce_{0.8}Gd_{0.2}O_{1.9}$-Ag cathode for ceria electrolyte SOFCs, Solid State Ionics 146 (2002) 203-210.

[17] V.V. Kharton, A.V. Kovalevsky, A.P. Viskup, F.M. Figueiredo, A.A. Yaremchenko, E.N. Naumovich, F.M.B. Marques, Oxygen permeability and Faradaic efficiency of $Ce_{0.8}Gd_{0.2}O_{2-\delta}$ -$La_{0.7}Sr_{0.3}MnO_{3-\delta}$ composites, J. Eur. Ceram. Soc. 21 (2001) 1763-1767.

[18] B. Wei, Z. Lü, S.Li, Y. Liu, K.Liu, W. Su, Thermal and electrical properties of new cathode material $Ba_{0.5}Sr_{0.5}Co_{0.8}Fe_{0.2}O_{3-\delta}$ for solid oxide fuel cells, Electrochem. Solid-State Lett. 8 (2005) A428-A431.
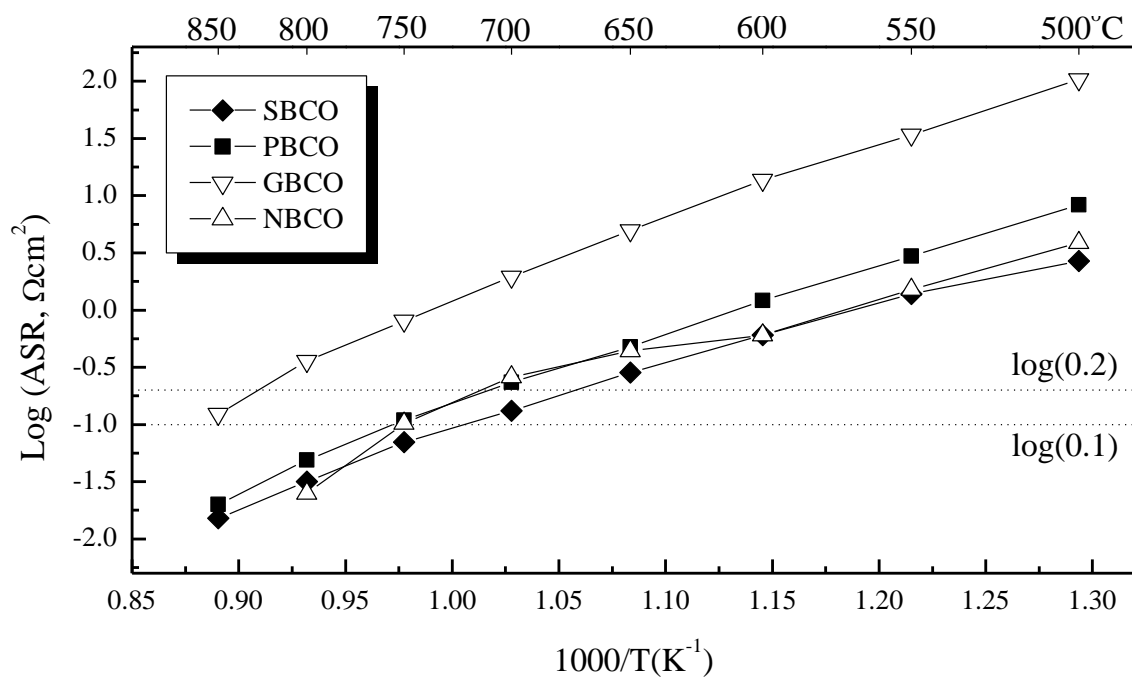
Fig. 1.

Fig. 1. Arrhenius plot of area specific resistances (ASRs) of $LnBa_{0.5}Sr_{0.5}Co_2O_{5+d}$ (Ln: Pr, Nd,
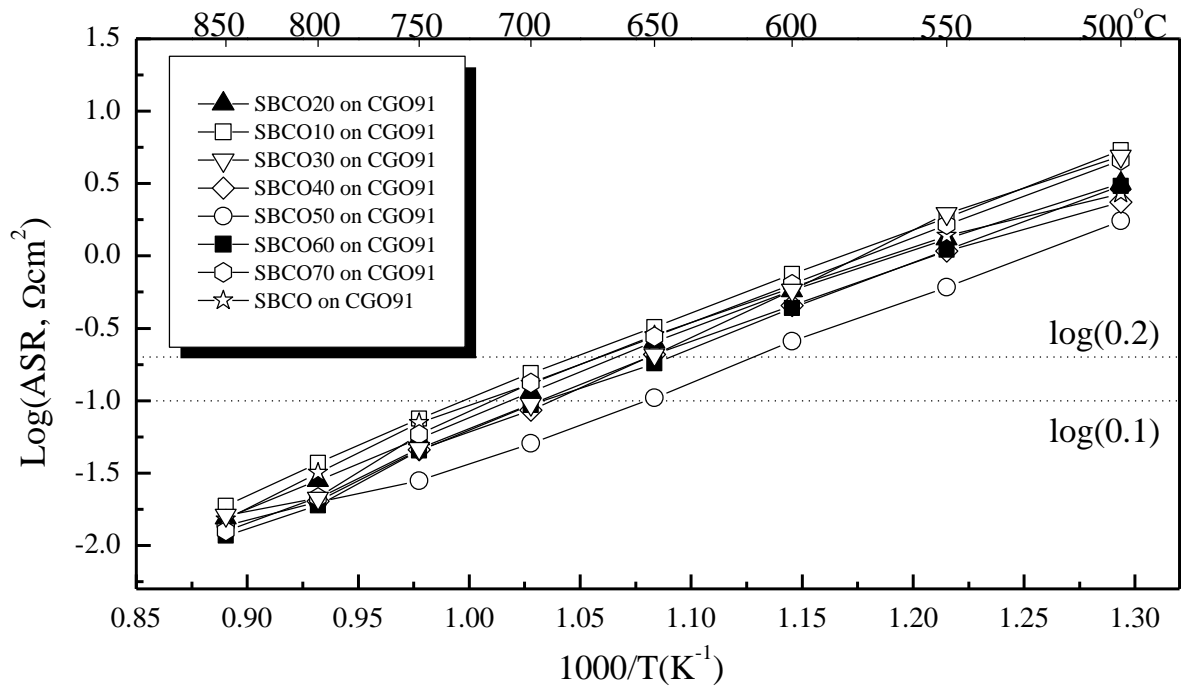
Sm and Gd) sintered at 1000 ^{o}C for 1 hour.

18

Fig. 2. (a)
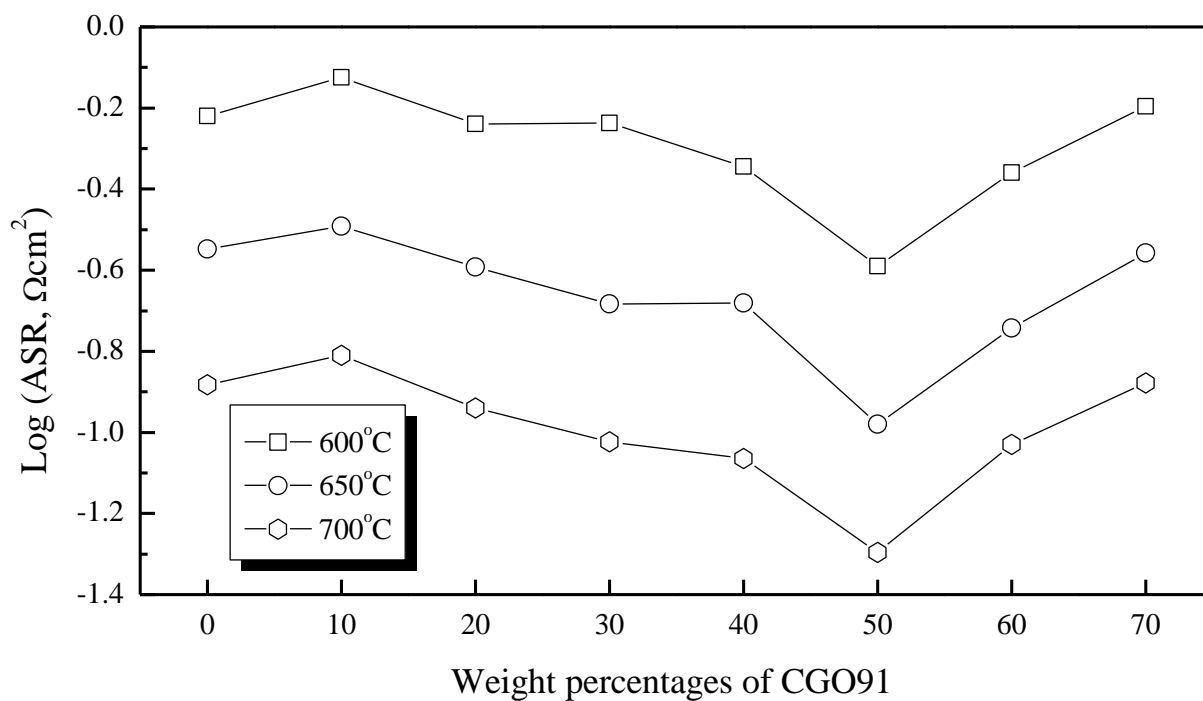
Fig. 2. (b)

Fig. 2. (a) Arrhenius plot of area specific resistances (ASRs) of composite cathodes with SmBaCo$_2$O$_{5+d}$ and CGO91 contents (0 wt% to 70 wt%) from 500 to 850 $^{\circ}$C and (b) summarized ASR results for composite cathodes with SmBaCo$_2$O$_{5+d}$ and CGO91 contents (0 wt% to 70 wt%) at 600, 650 and 700 $^{\circ}$C [7, 8].
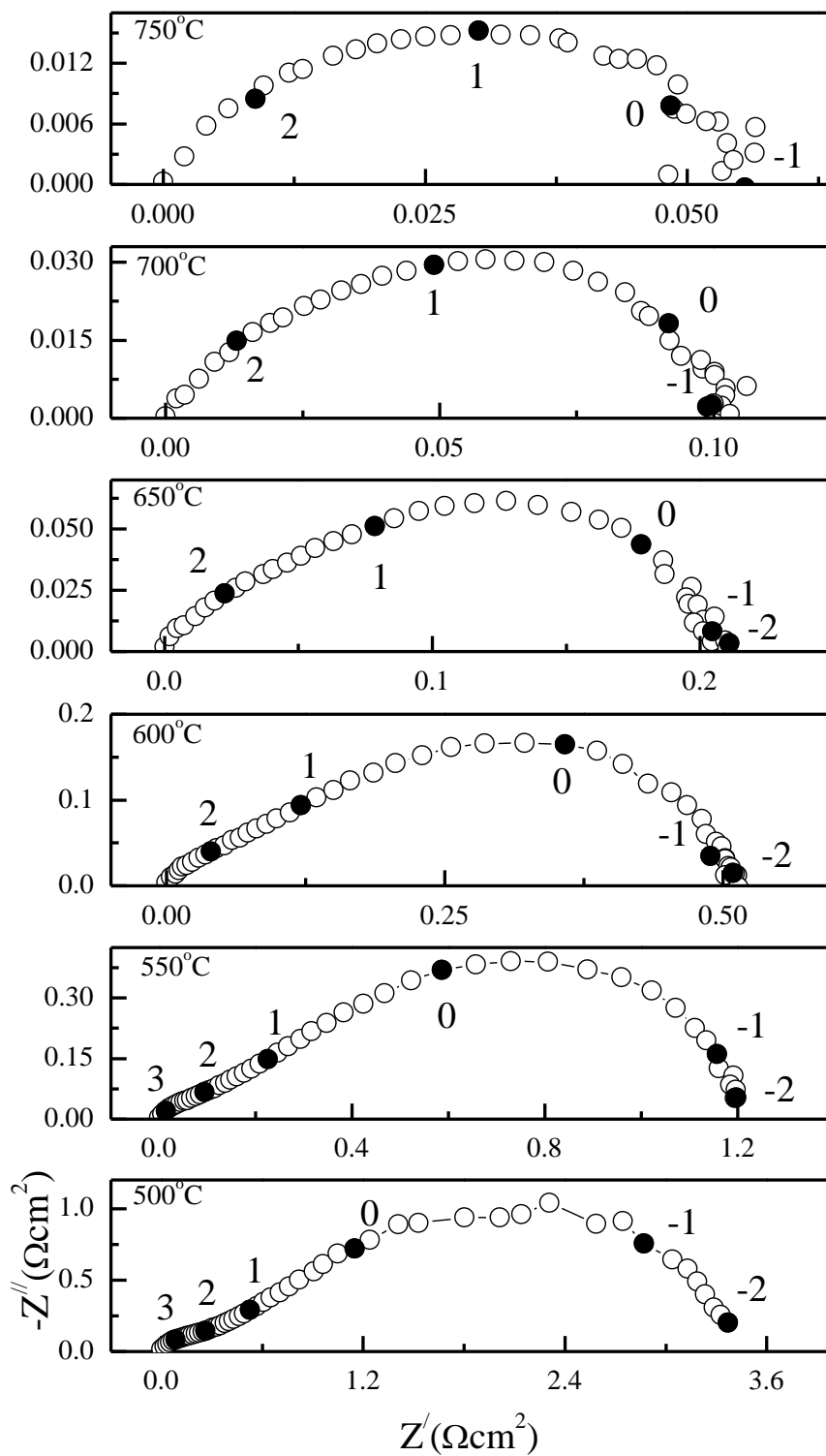
Fig. 3.

Fig. 3. Impedance plots of SBCO50 on CGO91 electrolyte from 200 to 750 °C. The inset

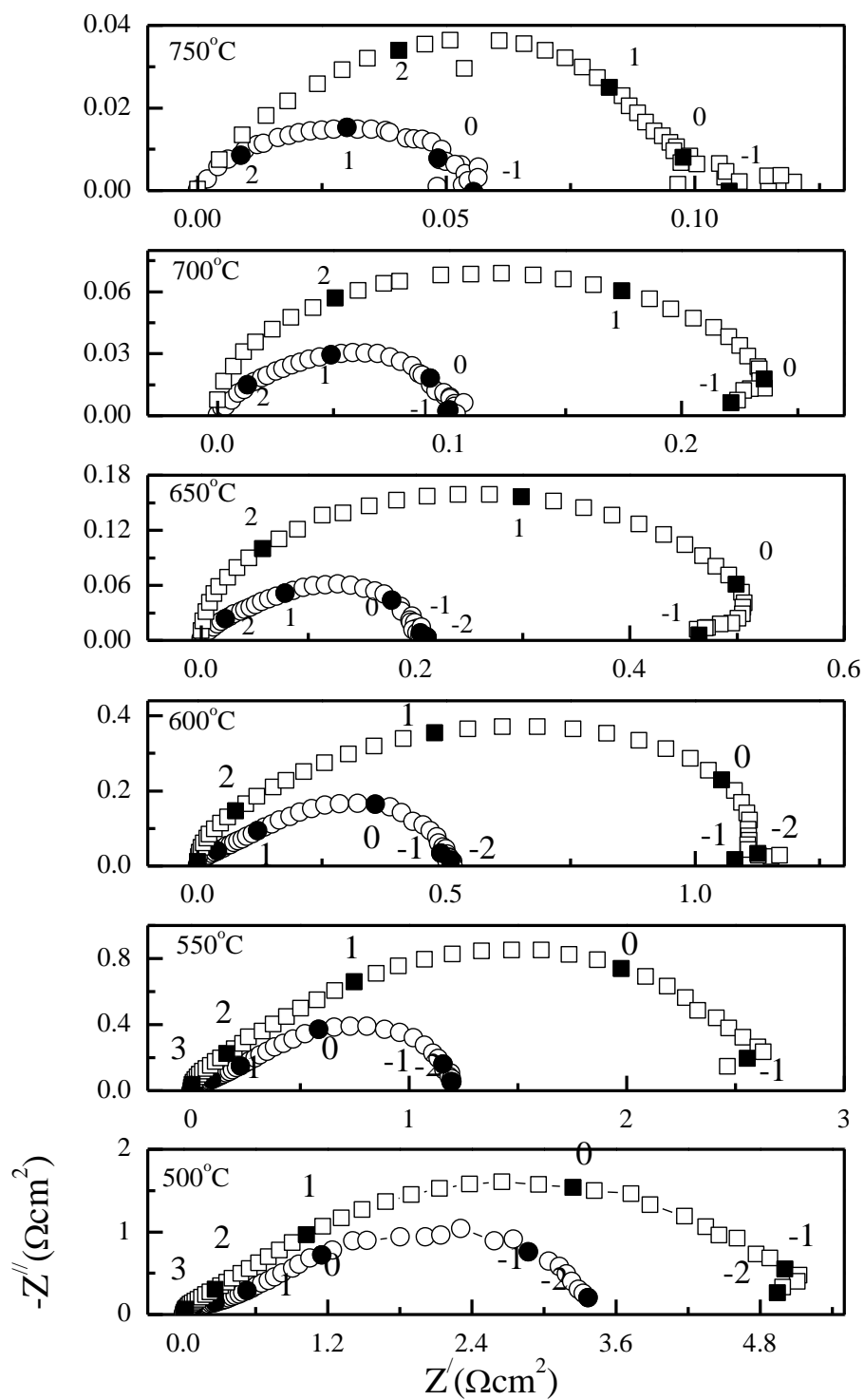numbers denote the logarithm of the measuring frequency.

Fig. 4.

Fig. 4. Comparison of impedance plots of SBCO50 and SBCO on CGO91 from 500 to 750 °C.

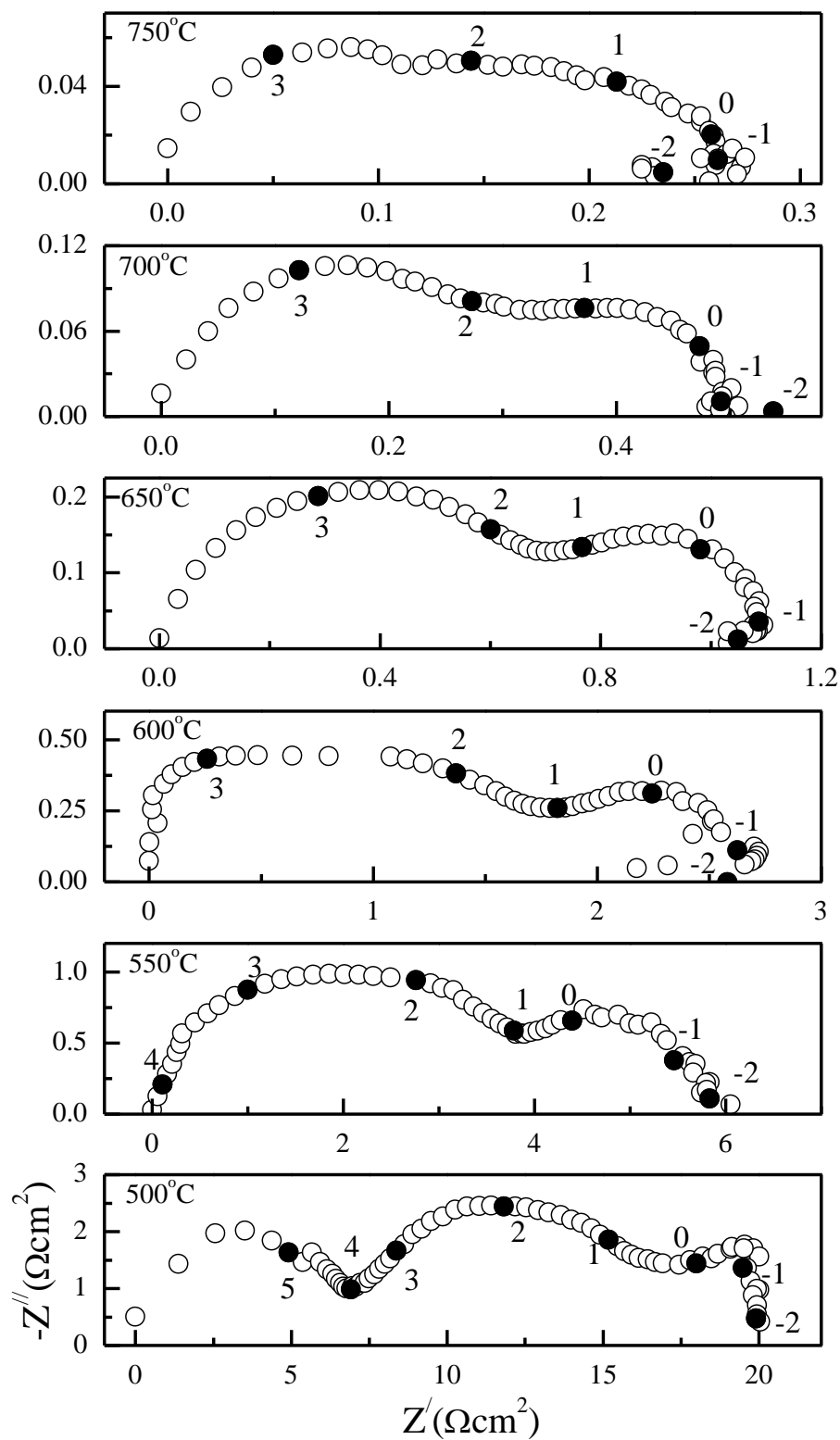The inset numbers denote the logarithm of the measuring frequency.

Fig. 5.

Fig. 5. Impedance plots of SBCO50 on CGO91 coated 8YSZ from 500 to 750 ^{o}C. The inset

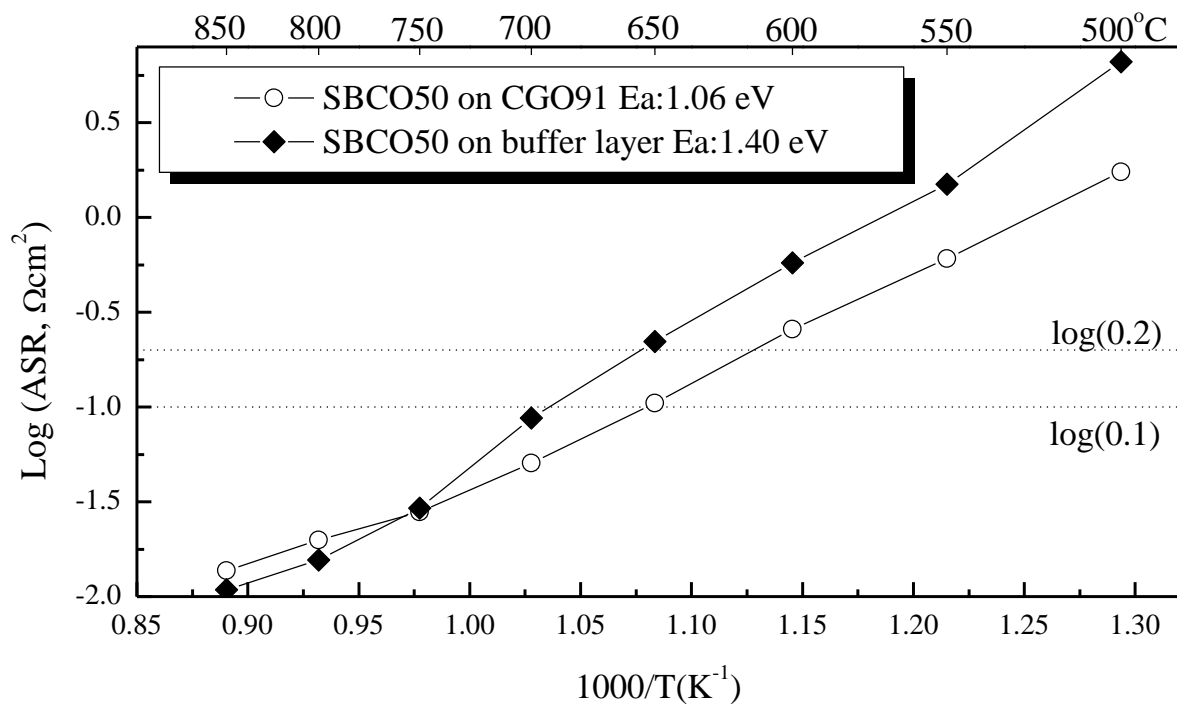numbers denote the logarithm of the measuring frequency.

23

Fig. 6.

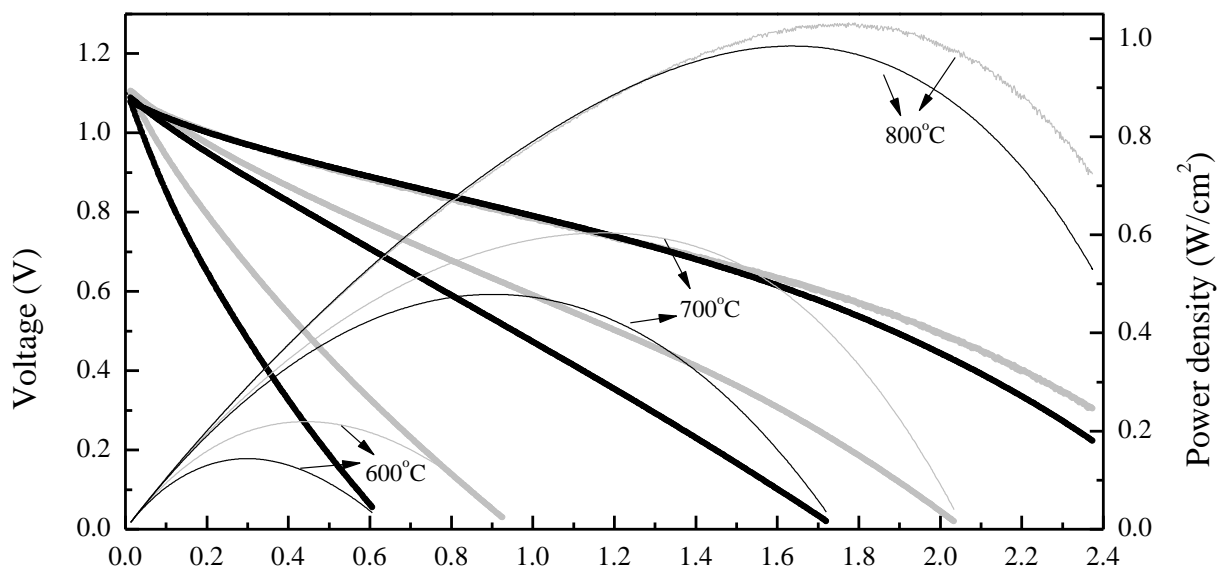Fig. 6. Comparisons of ASR results for SBCO50 on CGO91 and CGO91 (buffer layer) coated

8YSZ.

Fig. 7.

Fig. 7. Current (I) - voltage (V) - power density (P) curve of the Ni-YSZ / YSZ / CGO91 (buffer layer) / SBCO and Ni-YSZ / YSZ / CGO91 (buffer layer) / SBCO50 under 5% H_2 / N_2 as fuel and air as oxidant in the temperature range of 600 ºC to 800 ºC. The results expressed in gray color are from SBCO50 as a composite cathode; the black color shows the results for SBCO as single phase cathode.

Table 1. Chemical compositions and their initials in this research

Compositions	Initials
$PrBaCo_2O_{5+d}$	PBCO
$NdBaCo_2O_{5+d}$	NBCO
$SmBaCo_2O_{5+d}$	SBCO
$GdBaCo_2O_{5+d}$	GBCO
30 wt% SBCO and 70 wt% CGO91	SBCO70
40 wt% SBCO and 60 wt% CGO91	SBCO60
50 wt% SBCO and 50 wt% CGO91	SBCO50
60 wt% SBCO and 40 wt% CGO91	SBCO40
70 wt% SBCO and 30 wt% CGO91	SBCO30
80 wt% SBCO and 20 wt% CGO91	SBCO20
90 wt% SBCO and 10 wt% CGO91	SBCO10